

# Simultaneous Synthesis, Stabilization, and Self-Assembly of Microscale Drug Particles in Polymer Films

Xiangxin Meng,<sup>1</sup> Dachuan Yang,<sup>2</sup> Somenath Mitra<sup>1</sup>

<sup>1</sup>Department of Chemistry and Environmental Science, New Jersey Institute of Technology, Newark, New Jersey 07102

<sup>2</sup>Applied Science and Technology, Ethicon Research and Development, Somerville, New Jersey 08844

Received 19 October 2009; accepted 2 September 2010

DOI 10.1002/app.33342

Published online 8 December 2010 in Wiley Online Library (wileyonlinelibrary.com).

**ABSTRACT:** The antisolvent synthesis of micrometer-scale particles, their stabilization in suspension, and their subsequent self-assembly as homogeneous polymer films suitable for drug delivery were studied. Ultrasonic agitation was used in the precipitation of the drug particulates, stabilization was carried out with hydroxypropyl methylcellulose (HPMC), and finally, drug-encapsulated films containing HPMC and polyvinylpyrrolidone were synthesized. These contained as much 28% of the drug Griseoful-

vin, and the particles were distributed uniformly throughout the films. Most importantly, the redispersion of the drug-loaded films in an aqueous matrix showed that the crystallinity remained unaltered, and there was no appreciable increase in the particle size distribution. © 2010 Wiley Periodicals, Inc. *J Appl Polym Sci* 120: 2082–2089, 2011

**Key words:** drug delivery systems; films; nanotechnology; particle size distribution; stabilization

## INTRODUCTION

Potential drug molecules that exhibit poor aqueous solubility often end up as therapeutic failures.<sup>1</sup> Their insolubility is normally attributed to their inability to hydrogen bond with water and their high lattice energy.<sup>2</sup> Particle size reduction and incorporation within drug carriers are often used to increase the dissolution rate and bioavailability of such compounds. Conventional methods for the synthesis of micrometer/submicrometer particles include milling and homogenization, where the control of size, morphology, and surface properties are difficult.<sup>3</sup> Precipitation processes have emerged as effective methods for the synthesis of particulates of poorly water-soluble drugs. Typically, the molecule is first dissolved in a solvent and then mixed with a miscible antisolvent. This leads to the precipitation of microparticles/nanoparticles that may be directly incorporated into a drug-delivery vehicle.

Nucleation and growth need to be controlled to obtain micrometer and submicrometer particles dur-

ing a precipitation process. Polymers and surfactants are used as stabilizers to enhance colloidal stability.<sup>4–6</sup> Recently, we reported the use of cellulose ethers and surfactants, where appropriate combination enhanced the rate of particle formation and the reduction of the overall particle size.<sup>7</sup> In addition to providing colloidal stability, these materials can also be used for the synthesis of drug-delivery vehicles. Different celluloses such as hydroxypropyl methylcellulose (HPMC) and polymers such as chitosan have been used as biomaterials and microencapsulating agents. Although polymers such as poly(ethylene glycol) can serve as plasticizers, HPMC imparts a more hydrophilic characteristic and control of its porosity.<sup>8,9</sup> HPMC can be used in combination with a secondary polymer such as polyvinylpyrrolidone (PVP), which has good solubility in water and a variety of organic solvents. The latter can improve the wettability of the dispersed particles and, therefore, improve the dissolution rate. PVP also has good adhesive/binding properties, which help in the formation of a continuous matrix with the drug particles dispersed in it. PVP-based films have been fabricated for controlled delivery through the skin, and it has been reported that the release rates increase linearly with the PVP fraction. This was attributed to the leaching of PVP, which resulted in the formation of pores in films.<sup>10–12</sup>

These aqueous dispersions formed via antisolvent precipitation can be incorporated into a variety of final dosage forms, including biocompatible films, which have shown enormous potential.<sup>13,14</sup> Edible films dissolve rapidly in saliva without the need for water and, thereby, improve patient compliance and

Correspondence to: S. Mitra (somenath.mitra@njit.edu).

Contract grant sponsor: Center for Structured Organic Composites for Pharmaceutical, Nutraceutical, Agrochemical (National Science Foundation); contract grant number: EEC-0540855.

Contract grant sponsor: Nano Pharmaceutical, Engineering and Science (National Science Foundation); contract grant number: DGE-0504497.

acceptance. Films can also be designed to improve the onset of action for sublingual and buccal delivery and to provide controlled and sustained drug release and can be optimized on the basis of the mechanical properties, permeability, and water vapor transmission.<sup>15-17</sup>

The objective of this study was to integrate the antisolvent synthesis of micrometer-scale particles, their stabilization in aqueous suspensions, and the subsequent synthesis of polymer films for drug delivery. Our particular interest was in the antifungal agent Griseofulvin (GF), whose aqueous solubility is only 12  $\mu\text{g}/\text{mL}$ .

## EXPERIMENTAL

### Materials

GF (95% purity), HPMC (molecular weight = 10,000, viscosity = 5 cP), sodium dodecyl sulfate (SDS), and PVP 40 were purchased from Sigma Aldrich (St Louis, MO, USA). All of these materials were used without further purification. The water used in the experiments was purified with a Milli-Q Plus system.

### Preparation of stabilized drug suspensions and synthesis of drug-loaded polymer films and their redispersion

Antisolvent precipitation was carried out at room temperature. We prepared the antisolvent by dissolving HPMC in water. We prepared the solvent solution by dissolving GF in acetone. The mixing of antisolvent and solvent was carried out under ultrasonic agitation for 30 min. This was followed by 30 min of stirring to remove air bubbles. The film precursors were obtained by the addition of additional polymers, such as HPMC and PVP into the stabilized drug suspensions with stirring. A typical film suspension consisted of 0–6 wt % GF, 0–8 wt % HPMC, 0–20 wt % PVP, 0–0.2 wt % SDS, 60–85% antisolvent, and 0–25% solvent. Film suspensions were cast on Teflon plates and then dried at 40°C in a vacuum oven for 5 h and at room temperature for an additional 4 h. Finally, the films were peeled off and stored in a desiccator.

The films were redispersed after 4 months of storage. This was carried out by dissolution of the GF film in water, which was followed by 1 h of stirring.

### Characterization methods

Particle size analysis was carried out by static light scattering with a particle size analyzer LS230 (Beckman Coulter Inc., Miami, FL, USA). The atomic force microscopy (AFM) measurements were carried out with a Nanoscope II microscope (Digital Instruments Inc., Santa Barbara, CA, USA) in tapping mode at

room temperature ( $24 \pm 1^\circ\text{C}$ ). The film morphology was studied with a LEO 1530 VP scanning electron microscopy (LEO Electron Microscopy Inc., Thornwood, NY, USA). Samples were mounted on aluminum stubs with adhesive tape and coated with carbon with a MED 020 sputtering coater (Micro Surface Engineering Inc., Los Angeles, CA, USA) to improve conductivity. A Nicolet Almega XR Dispersive Raman with Olympus BX51 confocal microscope (Thermo Fisher Scientific Corp., Madison, WI, USA) with a laser at 532 nm was used to obtain the Raman spectra in the imaging mode. The samples were placed onto a glass slide for detection with a 100 $\times$  optical lens. X-ray diffraction (XRD) was used to investigate the crystallographic structure of the films. This was performed on a Philips X'Pert MRD X-ray diffractometer (Philips, Almedo, Netherlands) with Cu K $\alpha$  radiation operated at 45 kV and 40 mA. After redispersion, the particle size distribution (PSD) in the suspension was studied by static light scattering, and the dried GF particles were analyzed by XRD.

## RESULTS AND DISCUSSION

Antisolvent methods have been used in the synthesis of submicrometer and micrometer size particles of insoluble drug moieties.<sup>18,19</sup> Nucleation and condensation tend to be competing factors as both consume solute molecules, whereas the coagulation step involves aggregation.<sup>20-22</sup> The addition of stabilizer is known to slow the condensation and coagulation because of its lower Damköhler number.<sup>23</sup> Here we used cellulose ethers and surfactants to sterically stabilize the drug particles in the suspension; this prevented the water-insoluble particles from aggregating.<sup>24</sup> We examined several celluloses, including methylcellulose and hydroxyethyl cellulose, in our previous study, and HPMC was found to be the most suitable for stabilization.<sup>7</sup>

Initial attempts were aimed at increasing the concentration of cellulose ethers in the aqueous suspension and casting them as films. These did not form continuous films and were rather brittle. However, the addition of PVP led to the formation of stable, continuous films with reasonable mechanical properties. Therefore, both HPMC and PVP needed to be introduced into the suspension, which would eventually form a continuous film. We reported that the combination of HPMC and SDS is excellent for stabilizing a suspension of GF.<sup>7</sup> The goal was to introduce PVP into the suspension without a significant increase in particle size.

The mean diameter of particles in drug suspensions was measured with laser diffractometry, where both the Faunhofer and Mie theories were used to deduce PSD from spatial scattering.<sup>25</sup> The measurement in the submicrometer range was possible with

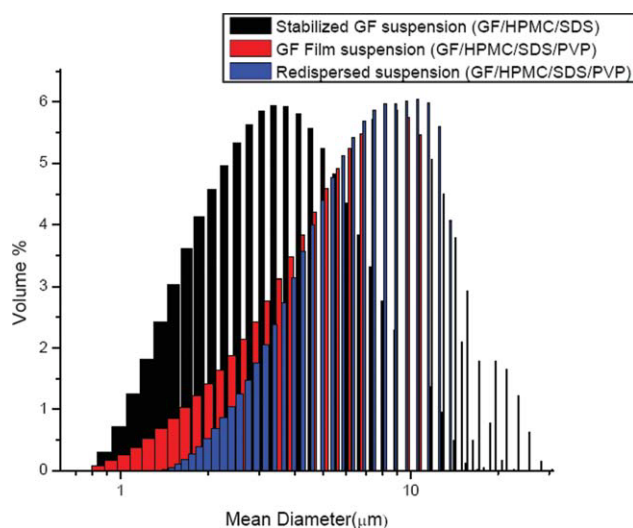


**Figure 1** PSDs of the suspensions: GF (0.41%) stabilized by HPMC (0.12%) and SDS (0.12 wt %) in suspension (black); GF (0.41%) stabilized by HPMC (0.82%), SDS (0.12%), and PVP (0.12 wt %) in suspension (red); and a redispersed suspension for the film cast from the GF suspension (blue). [Color figure can be viewed in the online issue, which is available at [wileyonlinelibrary.com](http://wileyonlinelibrary.com).]

a polarization intensity differential scattering system. Typical PSDs of the stabilized suspensions of GF in the HPMC/SDS and HPMC/SDS/PVP systems are shown in Figure 1. The latter contained higher amounts of HPMC and PVP and showed a shift toward a larger diameter. This was attributed to the higher concentrations of the polymers. Although there was a 35–70% increase in the mean particle diameter for the GF/HPMC/SDS/PVP systems, the diameter remained under 10  $\mu\text{m}$ . Furthermore, the effect of the concentration of HPMC and PVP during

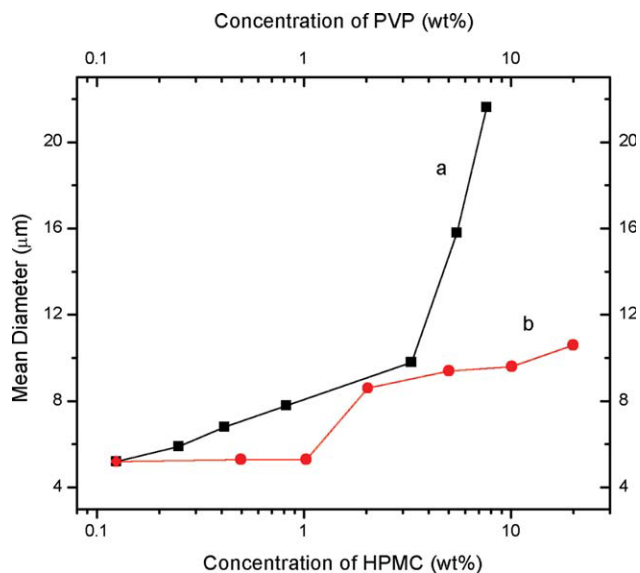


**Figure 2** Effect of the concentration of HPMC or PVP on the mean particle size: (a) the particle size as a function of the HPMC concentration and (b) the particle size as a function of the PVP concentration. The starting suspension had the following composition: 0.41% GF, 0.12% HPMC, 0.12% SDS, and 0.12 wt % PVP. [Color figure can be viewed in the online issue, which is available at [wileyonlinelibrary.com](http://wileyonlinelibrary.com).]

the antisolvent precipitation on the particle size in the suspensions was examined, and the results are shown in Figure 2. With the increase in the concentration of HPMC, the particle size in the suspension increased, and the effects were quite pronounced. The particle size remained relatively constant below 1.0 wt % PVP, but beyond that, there was a marked increase. The average particle size increased to as high as 20  $\mu\text{m}$ . The increase was attributed to the fact that at high PVP and HPMC concentrations, the

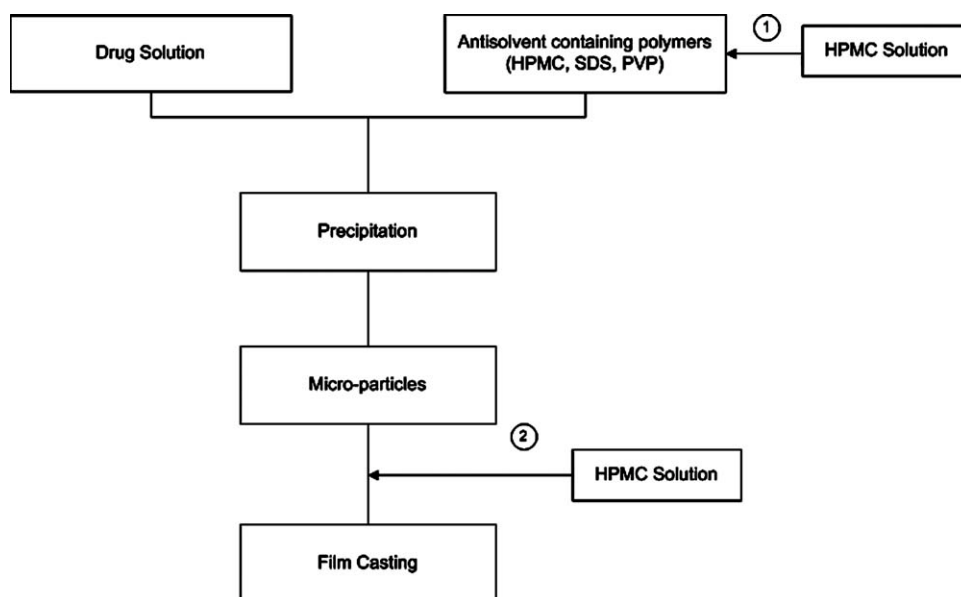


**Figure 3** Approach to integrating antisolvent precipitation and film casting.

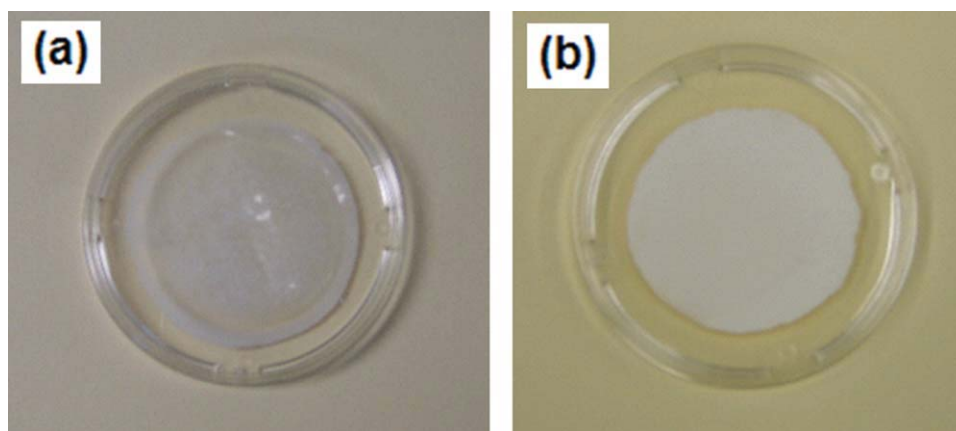


**Figure 4** Photographs of films: (a) a blank polymer film and (b) a GF-loaded polymer film. [Color figure can be viewed in the online issue, which is available at [wileyonlinelibrary.com](http://wileyonlinelibrary.com).]

degree of supersaturation decreased and led to a low nucleation rate and larger particles.

At higher polymer concentration in the suspensions, there was a marked phase separation as the polymers began to precipitate. As shown in Figure

2, high concentrations of HPMC affected the particle size in the suspension and, finally, in the films. The film formation was carried out according to Figure 3. The HPMC could be added either at stage 1 or stage 2, when particles were already stabilized. On

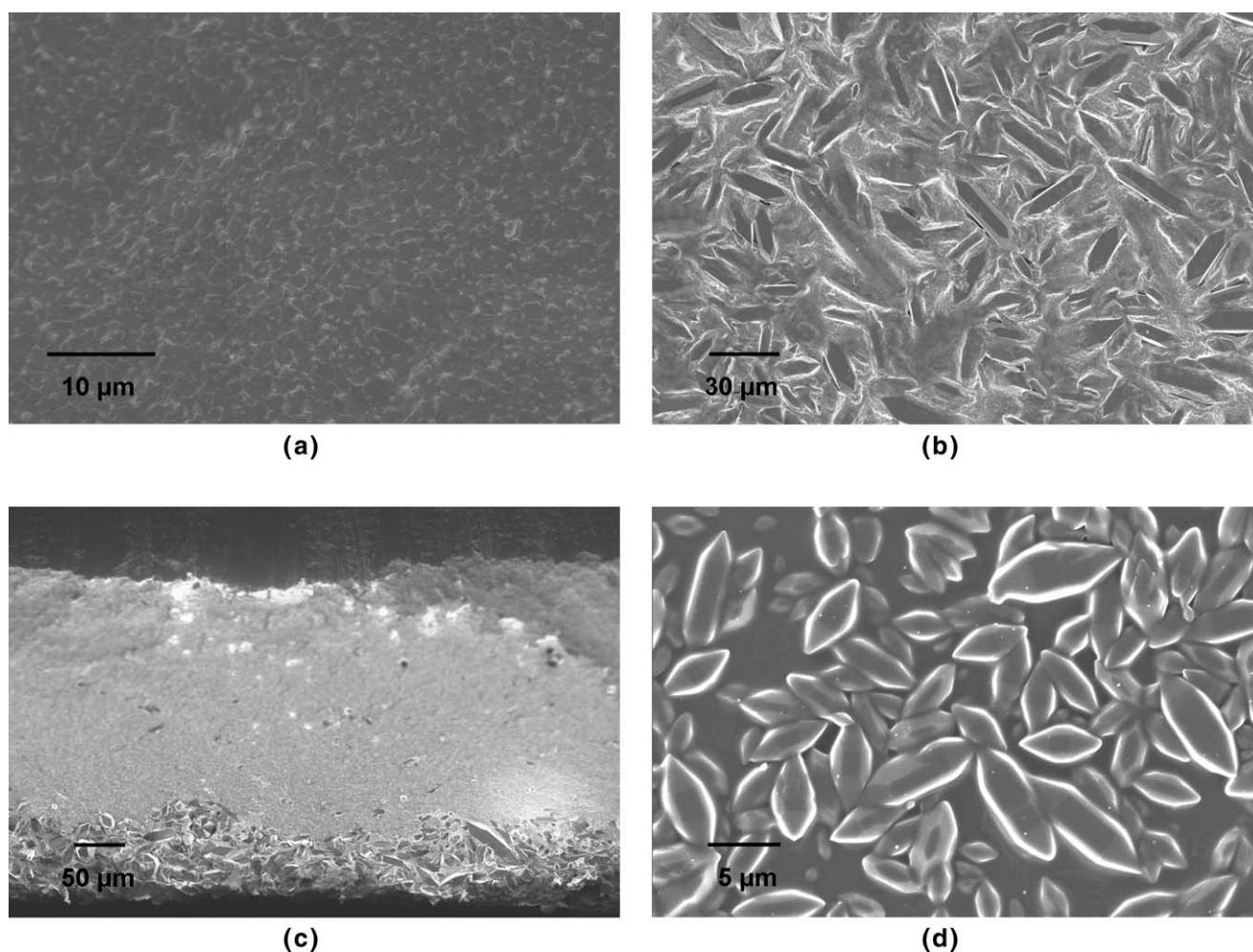


**Figure 5** SEM images of a GF-loaded polymer film (film A) containing 6.2% GF, 84.3% HPMC, and 5.9% PVP: (a) top surface, (b) bottom surface, (c) cross section, and (d) GF particles in a redispersed suspension.

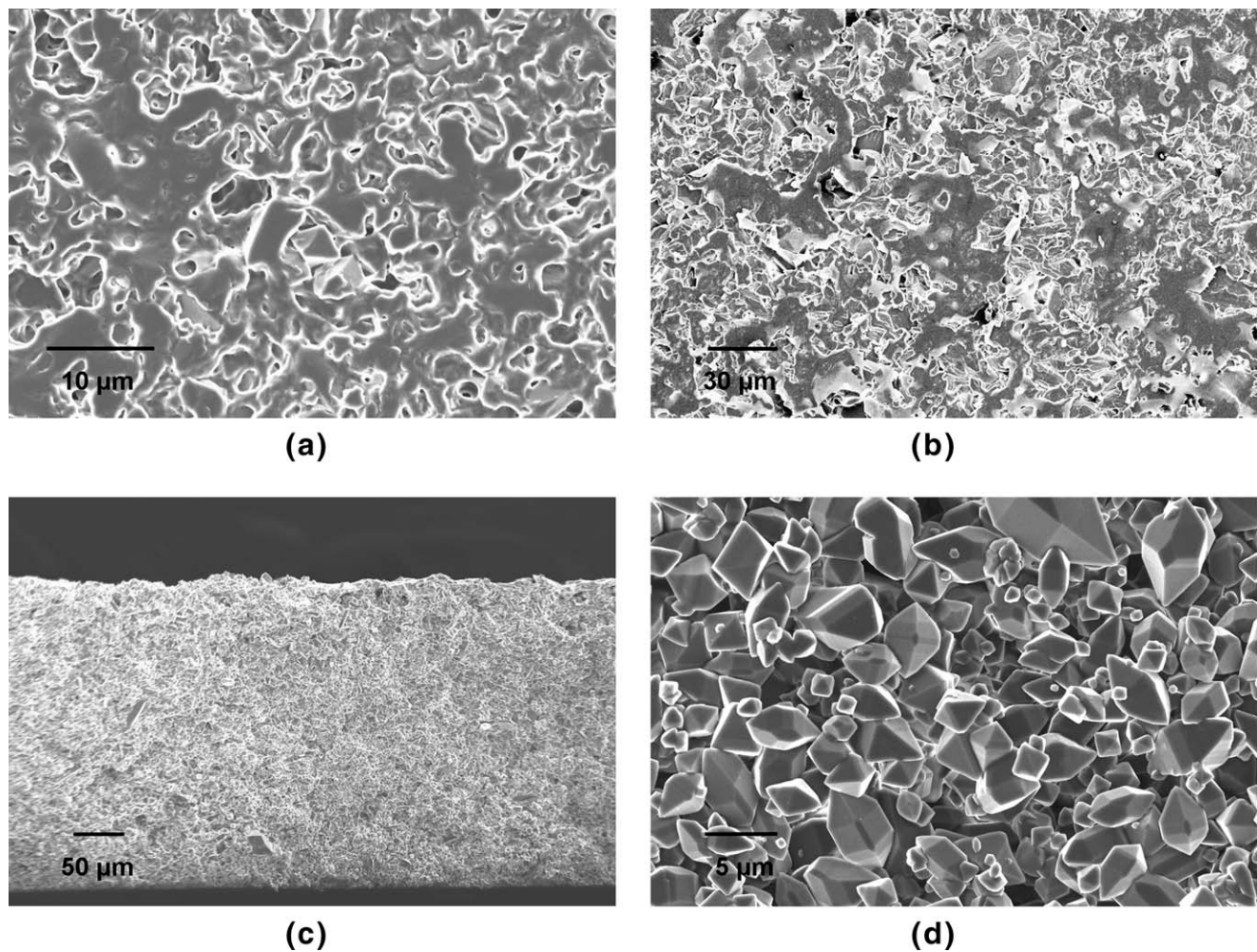


**Figure 6** SEM images of a GF-loaded polymer film (film B) containing 27.8% GF, 55.6% HPMC, and 10.3% PVP: (a) top surface, (b) bottom surface, (c) cross section, and (d) GF particles in a redispersed suspension.

the basis of Figures 1 and 2, stage 2 was selected, and it led to a smaller particle size.

As mentioned before, the absence of PVP led to the formation of brittle films that were not uniform,

where the drug particles and the polymers separated during film formation. The blank film was transparent in color, as shown in Figure 4, whereas the one containing the drug was white with a different

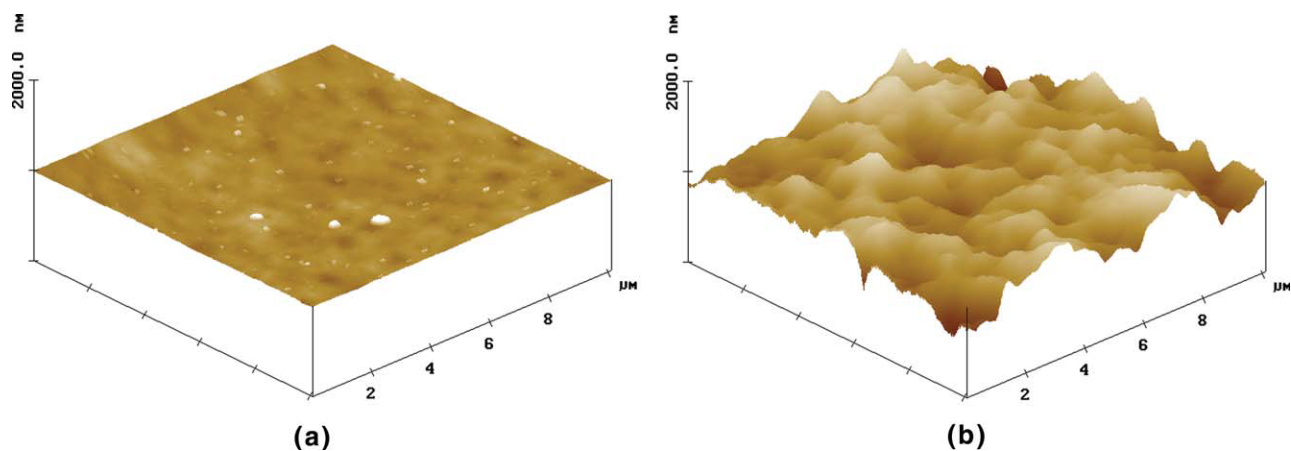


**Figure 7** Tapping-mode, two-dimensional AFM images of top surfaces (10- $\mu\text{m}$  scans): (a) a non-drug-loaded polymer film and (b) film B. [Color figure can be viewed in the online issue, which is available at [wileyonlinelibrary.com](http://wileyonlinelibrary.com).]

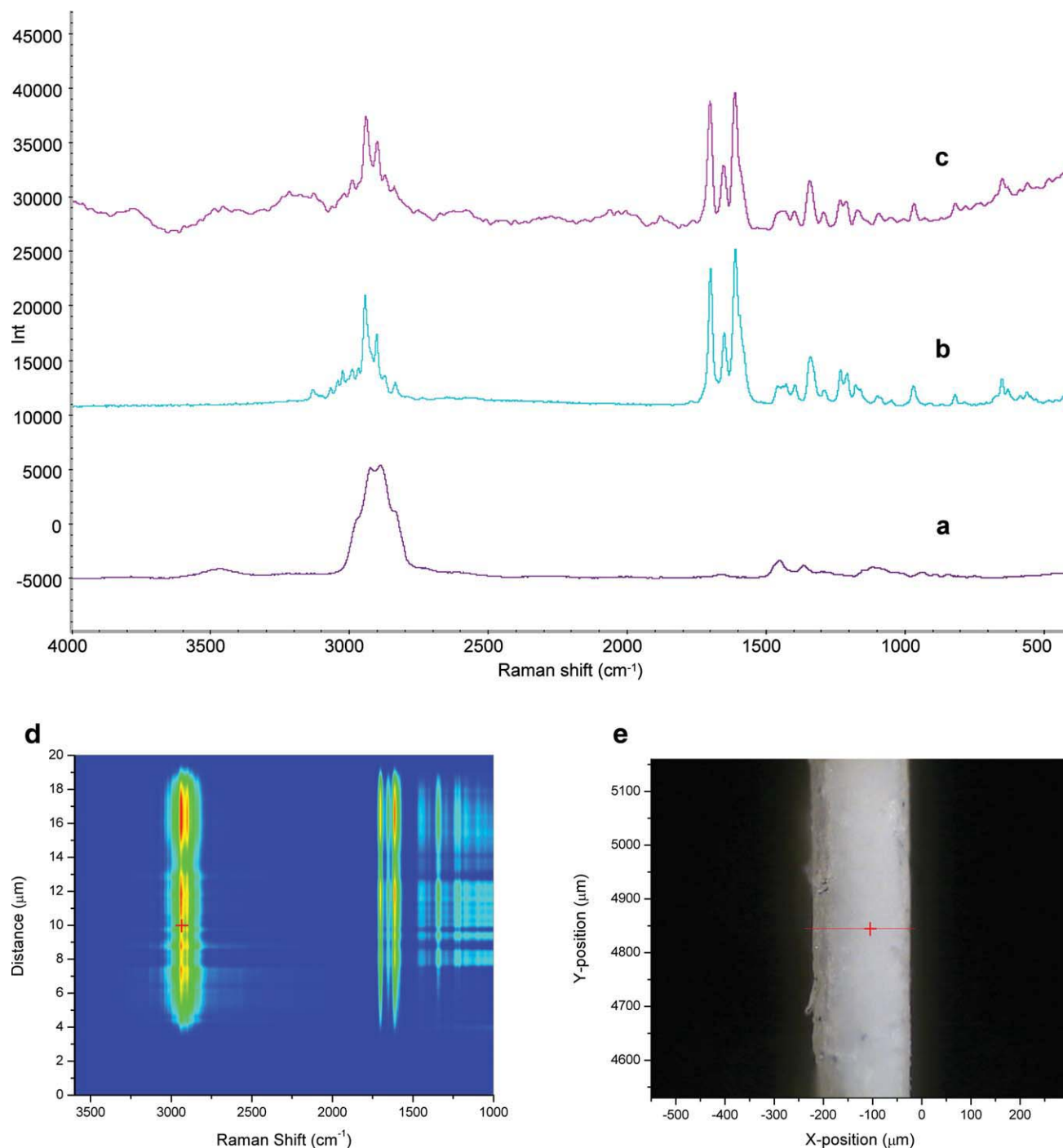


**Figure 8** Cross section of film B containing 27.8% GF: (a–c) Raman spectra of a blank film, pure GF, and film B, respectively; (d) Raman line mapping; and (e) a Raman real image. Scanning was performed at 1699 cm<sup>-1</sup>. [Color figure can be viewed in the online issue, which is available at [wileyonlinelibrary.com](http://wileyonlinelibrary.com).]

texture. The thickness of the drug-loaded films could be varied, but in this study, we targeted between thicknesses between 300 and 400 μm. The PVP was the binder used in these films, and no phase separation was observed. A film containing between 5 and 20% (on a dry basis) of PVP showed good uniformity and mechanical properties. The HPMC–PVP combination was a good one because the ether and

hydroxyl groups of HPMC could interact with the imide and carbonyl groups of PVP via hydrogen bonding.<sup>26</sup>

SEM was used to study the surface morphology and GF particle distribution within the films. The goal was to obtain a uniform distribution of GF particles throughout the film. Figure 5(a–c) show SEM images of the GF-loaded film containing 6.2% GF,

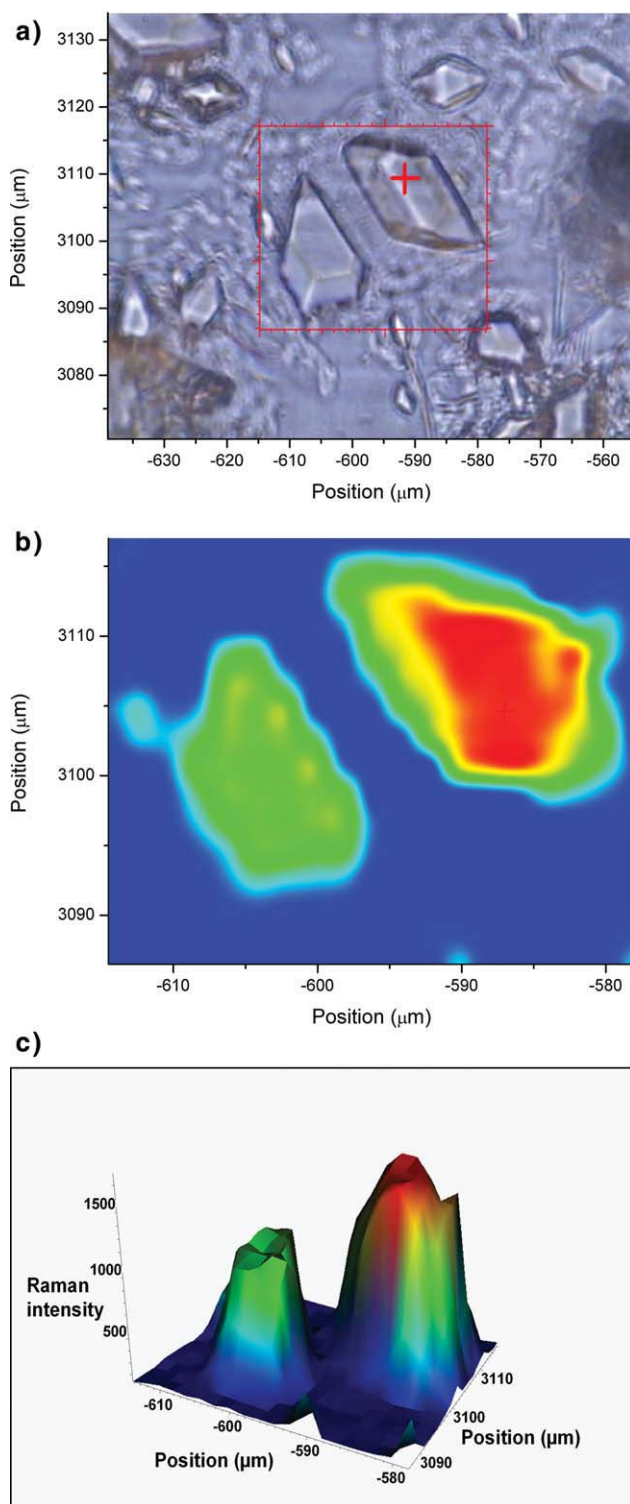


**Figure 9** Raman mapping of the drug particles on the surface of a GF-loaded polymer film containing 3.7% GF: (a) a microscopic photograph of the scanned area, (b) the GF distribution in the scanned area (two-dimensional; the blue area corresponds to a non-GF background, and the green and red areas correspond to a high GF concentration); and (c) three-dimensional chemical imaging of the scanned area. Scanning was performed at  $1699\text{ cm}^{-1}$ . [Color figure can be viewed in the online issue, which is available at [wileyonlinelibrary.com](http://wileyonlinelibrary.com).]

84.3% HPMC, 5.9% PVP, and 3.6% SDS. This film is referred to as film A. The distribution of particles was found to be nonuniform. The top surface showed mainly the presence of polymer, whereas the GF particles settled to the bottom surface. Figure 6(c) shows the SEM of the cross section and nonhomogeneous distribution of GF. This was typical when the HPMC concentration was high. The SEM images of the surface, bottom, and cross section of the GF-loaded film containing a lower concentration of HPMC and a relatively higher concentration of PVP are shown in Figure 6(a–c) (film B). It contained 27.8% GF, 55.6% HPMC, 10.3% PVP, and 6.3% SDS. In film B, the particles were uniformly distributed. Both the top surface and bottom surface showed the presence of a large number of GF crystals. SEM of the cross section showed that the drug particles were uniformly distributed throughout the film.

The surface topography of the non-drug-loaded polymer film and film B were analyzed by AFM in the tapping mode (Fig. 7). The blank film with no drug loading showed a smooth surface with a average roughness ( $R_a$ ) of 2.8 nm, whereas that for film B was 91.3 nm. This indicated the presence of drug particles on the film surface. Similar images were also obtained for other drug films containing different concentrations of GF. The images showed consistency with previous results obtained by SEM measurements, which showed that the drug particles were embedded into the film. The presence of drug particles also altered the surface morphology.

Raman spectroscopy was used to image the films and the concentration distribution of GF. It provided sensitive GF detection in the excipient matrices, and the well-resolved fundamental intramolecular and/or intermolecular stretching and bending modes

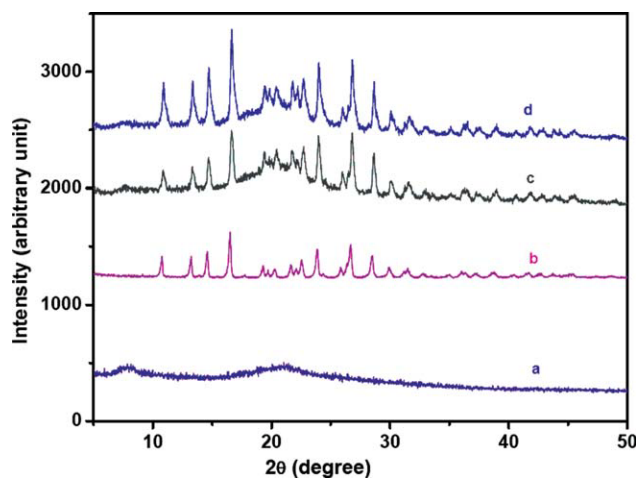


**Figure 10** XRD patterns of (a) a blank polymer film, (b) pure GF, (c) film B containing 27.8% GF, and (d) redispersed particles. [Color figure can be viewed in the online issue, which is available at [wileyonlinelibrary.com](http://wileyonlinelibrary.com).]

allowed determination in the solid state. Figure 8(a–c) shows the Raman spectra of the blank film, GF-loaded film (film B, containing 27.8% GF), and pure GF, respectively. The GF spectra showed strong peaks in the regions 1550–1800 and 2800–3200  $\text{cm}^{-1}$ ; these peaks were attributed to the C=O stretching of the benzofuran ring and C–H stretching of GF, respectively.<sup>27</sup> The same characteristic peaks were also observed in film B, which indicated the presence of the drug and no significant alteration of the GF molecule.

Raman chemical mapping was used to image the cross section of film B. The chemical images corresponding to 1699  $\text{cm}^{-1}$  were attributed to GF. Figure 8(d,e) shows uniform distribution of the drug. The images were consistent with the SEM measurements. The Raman spectroscopy was also able to map the GF concentration in three dimensions. A film containing only 3.7% GF is shown Figure 9. Two particles embedded in the film were mapped, and Figure 9(a–c) shows the distribution of GF. We did this by plotting the peak area of the selected Raman bands over the entire scanned area. Red corresponds to a high GF concentration, followed by yellow and green, whereas blue signifies the background. The strongest Raman bands of GF were identified in the center of the particles; these decreased away from the central core. This indicated that the drug was coated and distributed in the polymer matrix. Similar results were obtained for different GF films with different GF concentrations. These observations agreed with the SEM measurements and suggested that drug existed in the form of microparticles dispersed in the polymer matrix.

XRD analysis was used to study the crystal structure of GF in the film (Fig. 10). The crystal structure did not change when the stabilized particles were embedded in the polymer matrix. The spectra of pure GF and the GF-loaded polymer film were identical, and neither splitting nor shifting of the peak was observed for the GF-loaded polymer film; this indicated that there was no change in polymorphism.

The GF films were stored at room temperature for 4 months before redispersion in aqueous medium. The PSD of the redispersion was studied and is shown in Figure 1. It is evident that the size distribution was not altered significantly. SEM analysis [Fig. 5(d) and 6(d)] of the dried GF particles from the redispersions of film A and B showed similar crystal shapes to the original particles. The XRD pattern of particles from the redispersion of film B showed that the pattern remained unchanged [Fig. 10(d)]. Therefore, we concluded that the multiple steps of film formation, storage, and redispersion did not alter the properties of the drug, including its crystallinity.

## CONCLUSIONS

The integration of the antisolvent synthesis of micrometer-scale particles, their stabilization in suspension, and subsequent film formation were accomplished. Although HPMC was an excellent at stabilizing GF in suspension, PVP was necessary to make continuous films that contained a uniform distribution of GF particles. The main particle sizes in the suspension and the solids films were between 1 and 10  $\mu\text{m}$ .

The authors thank Rajesh Dave for his help and assistance on various levels.

## References

1. Gao, Y.; Li, L.; Zhai, G. *Colloids Surf B* 2008, 64, 194.
2. Kipp, J. E. *Int J Pharm* 2004, 284, 109.
3. Wong, S. M.; Kellaway, I. W.; Murdan, S. *Int J Pharm* 2006, 317, 61.
4. Terayama, H.; Funakoshi, M.; Torigoe, K.; Esumi, K. *Colloids Surf B* 2002, 23, 65.
5. Itoh, K.; Pongpeerapat, A.; Tozuka, Y.; Oguchi, T.; Yamamoto, K. *Chem Pharm Bull* 2003, 51, 171.
6. Yasueda, S.; Inada, K.; Matsuhisa, K.; Terayama, H.; Ohtori, A. *Eur J Pharm Sci* 2004, 57, 377.
7. Meng, X.; Chen, Y.; Chowdhury, S. R.; Yang, D.; Mitra, S. *Colloids Surf B* 2009, 70, 7.
8. Fulzele, S. V.; Satturwar, P. M.; Dorle, A. K. *Int J Pharm* 2002, 249, 175.
9. Zili, Z.; Sfar, S.; Fessi, H. *Int J Pharm* 2005, 294, 261.
10. Ye, Z.; Rombout, P.; Remon, J. P.; Vervaet, C.; Mooter, G. V. *Eur J Pharm Biopharm* 2007, 67, 485.
11. Rao, P. R.; Diwan, P. V. *Drug Dev Ind Pharm* 1998, 4, 327.
12. Zhang, T. R.; Lu, R.; Liu, X. L.; Zhao, Y. Y.; Li, T. J.; Yao, J. N. *J Solid State Chem* 2003, 172, 458.
13. Schmidt, C.; Bodmeier, R. *J Controlled Release* 1999, 57, 115.
14. Zheng, W.; Sauer, D.; McGinity, J. W. *Eur J Pharm Biopharm* 2005, 59, 147.
15. Akhgari, A.; Farahmand, F.; Afrasiabi Garekani, H.; Sadeghi, F.; Vandamme, T. F. *Eur J Pharm Sci* 2006, 28, 307.
16. Shogren, R. *J Environ Polym Degrad* 1997, 5, 91.
17. Nagarsenkar, M. S.; Hegde, D. D. *Drug Dev Ind Pharm* 1999, 25, 95.
18. Giannidis, B. D.; Jestin, P.; Subra, P. *J Cryst Growth* 2004, 262, 519.
19. Zimmermann, A.; Elema, M. R.; Hansen, T.; Mullertz, A.; Hovgaard, L. *J Pharm Biomed* 2007, 44, 874.
20. Weber, M.; Russell, L. M.; Debenedetti, P. G. *J Supercrit Fluid* 2002, 23, 65.
21. Young, T. J.; Johnston, K. P.; Pace, G. W.; Mishra, A. K. *AAPS PharmSciTech* 2003, 5, 1.
22. Marchisio, D. L.; Rivautella, L.; Barresi, A. A. *AIChE J* 2006, 52, 1877.
23. Matteucci, M. E.; Hotze, M. A.; Johnston, K. P.; William, R. O. *Langmuir* 2006, 22, 8951.
24. Ain-Ai, A.; Gupta, P. K. *Int J Pharm* 2008, 351, 282.
25. Larson, J. R.; Gibson, G. A.; Schmidt, S. P. In *Handbook of Imaging Materials*; Diamond, A. S.; Weiss, D. S., Eds.; Marcel Dekker: New York, 2002; p 239.
26. Chan, L. W.; Ong, K. T.; Heng, P. W. S. *Pharm Res* 2005, 22, 476.
27. Bolton, B. A.; Prasad, P. N. *J Pharm Sci* 1981, 70, 789.